2000-01-0865

Experimental Approach to Optimize Catalyst Flow Uniformity

Michael Breuer and Christof Schernus
FEV Motorentechnik GmbH

Robert Böwing
Aachen University of Technology

André Kuphal and Stefan Lieske
Volkswagen AG

GLOBAL MOBILITY DATABASE

All SAE papers, standards, and selected books are abstracted and indexed in the Global Mobility Database

Printed in USA

Experimental Approach to Optimize Catalyst Flow Uniformity

Michael Breuer and Christof Schernus
FEV Motorentechnik GmbH

Robert Böwing
Aachen University of Technology

André Kuphal and Stefan Lieske
Volkswagen AG

ABSTRACT

A uniform flow distribution at converter inlet is one of the fundamental requirements to meet high catalytic efficiency. Commonly used tools for optimization of the inlet flow distribution are flow measurements as well as *CFD* analysis. This paper puts emphasis on the experimental procedures and results. The interaction of flow measurements and *CFD* is outlined.

The exhaust gas flow is transient, compressible and hot, making in-situ flow measurements very complex. On the other hand, to utilize the advantages of flow testing at steady-state and cold conditions the significance of these results has to be verified first. *CFD* analysis under different boundary conditions prove that - in a first approach - the flow situation can be regarded as a sequence of successive, steady-state situations. Using the Reynolds analogy a formula for the steady-state, cold test mass flow is derived, taking into account the cylinder displacement and the rated speed.

At cold test conditions the flow field downstream of the converter is visualized by *Particle Image Velocimetry (PIV)* in terms of planar velocity fields. The flow structure is shown to be significantly one-dimensional. Therefore a single hot wire probe is sufficient to scan the axial component directly at converter outlet. Results of *PIV* and *Hot Wire Anemometry (HWA)* are compared.

The planar mass flow distribution downstream catalyst is essential to analyze and optimize the exhaust system upstream of the converter. Nevertheless, to quantify the success of a geometric modification a more condensed result is favorable. In this paper the velocity density function is presented as a helpful method to characterize the flow uniformity. Furthermore it is shown that this distribution curve contains both characteristic numbers, which are commonly used to quantify catalyst flow distribution. This method is applied to a typical *HWA* result.

INTRODUCTION

In Figure 1, different tools to analyze and optimize catalyst flow uniformity are arranged in a plane, built up by their spatial and temporal resolution. The notation yC/rD indicates that y components of the *3D* velocity vector C are caught in an r-dimensional area D. Moreover, the figure displays whether the investigations are carried out at fired or at cold test conditions. The interactions of the analysis tools are subdivided into providing boundary conditions and enabling verifications.
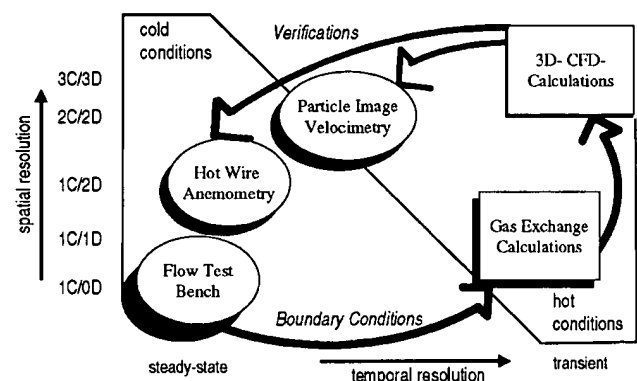
Figure 1. Characterization and Interaction of different Flow Analysis Tools

At the *flow test bench* the discharge coefficients of the exhaust system are measured at cold, steady flow conditions. These data serve as input for 1D *gas exchange calculations*, taking into account the wave phenomena in all tubes of the intake and exhaust system. The calculated pressure traces are impressed on the fluid borders of the *CFD calculation* grid. To close the circle of interdependencies the *CFD* outcome at steady conditions is verified by *PIV-* and *HWA-* results.

This paper describes some of the analysis tools, proves the significance of steady-state experiments, presents typical results and explains an instructive method to assess the flow uniformity.

STEADY FLOW TESTING

Gas exchange calculations as well as *CFD* codes demand information about flow resistance of the catalytic system. Usually the discharge coefficient is derived from steady flow testing at cold conditions. According to the laws of similarity at low Mach numbers *(Ma<0,5)* the result must have the form

$$Eu = f(Re); \ Eu = \frac{\Delta p}{\rho c^2}; \ Re = \frac{cD}{\nu}$$

{1}

To ensure comparable flow structures at different temperature levels, the mass flow has to be adjusted to identical *Re* numbers. According to {1}, this will effect the same *Eu* numbers.

Figure 2 elucidates the relations at constant *Re* numbers. The kinematic viscosity n of air grows up with temperature *T* according to

$$\frac{\nu_2}{\nu_1} = \left(\frac{T_2}{T_1}\right)^{1,63}$$

{2}

If $T_2 < T_1$, the mass flow has to be reduced to keep *Re* constant. At the same time, flow velocities (c_2/c_1), *Ma* number (Ma_2/Ma_1) and pressure losses $(\Delta p_2/\Delta p_1)$ will get smaller.
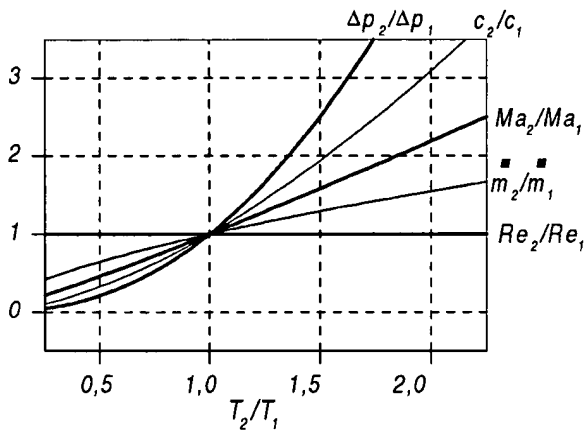

Figure 2.   *Re* Analogy

Thus, the mass flow rate at cold conditions can be reduced compared to the fired engine operation. Although the *Eu* number remains constant, the pressure drop at cold conditions is significantly lower. These relations must be considered, if the flow results are used for gas exchange calculations.

GAS EXCHANGE CALCULATIONS

In principle, the calculation model is built up by non-dimensional elements with (e.g. intake plenum, cylinder, muffler) or without mass capacity (e.g. tube junctions, cross section bounds) and one-dimensional tubes (e.g. intake runner, exhaust runner). In the tubes all non-linear wave phenomena are simulated.

In particular this tool is used to determine the instantaneous pressure and mass flow traces downstream of the outlet valves as well as downstream of the catalyst.
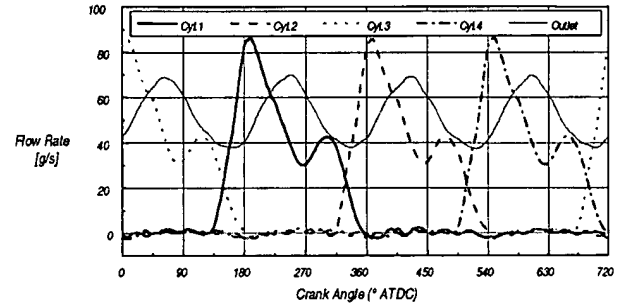

Figure 3.   Calculated Mass Flow Traces at Exhaust Manifold Flange

According to Figure 3 two characteristic mass flow peaks can be distinguished: *blowdown phase*, where cylinder pressure reduces towards exhaust gas backpressure – and *displacement phase*, which is provoked by the maximum piston velocity. The highest flow rate typically causes the most critical flow patterns in the converter due to stall and choked flow effects. Therefore, the peak rate is chosen as boundary condition for the further investigations /2/.

CFD CALCULATIONS

The exhaust manifold is modeled from cylinder head flange downstream to the outlet of the converter, Figure 4. At the boundaries of the model results from one-dimensional gas exchange calculation, e.g. temperature and pressure or flow rate, are imposed as boundary conditions.

The mesh size depends on the volume and the shape of the manifold. Typically, between 70000 and 300000 hexahedral cells are used to discretize the inner volume of manifold and converter. The catalytic converter itself is represented by a porous media with permeability only in the direction of the converter channels.
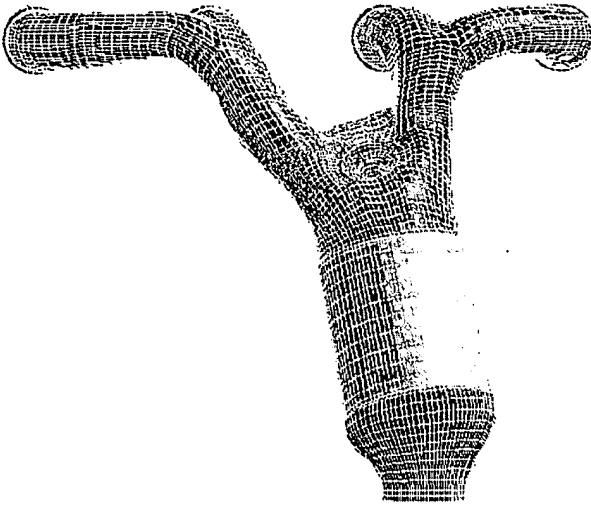
2

Figure 4. *CFD* Calculation Grid /1/

Figure 5 shows the velocity distribution in the frontal area of the catalytic converter. Here flow goes through each exhaust runner separately, while flow rate corresponds to the peak rates according to Figure 3. The flow profile on the catalyst matrix significantly varies along with the mass flow load from the single cylinder runners.
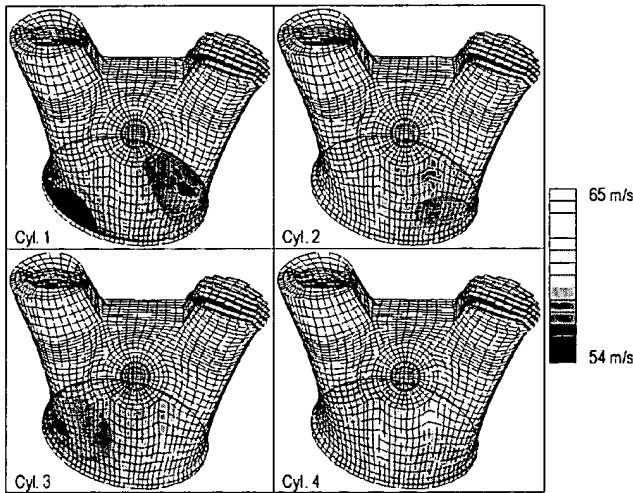

Figure 5. *CFD* Flow Distribution at Catalyst Inlet

In this form however, a verification of the *CFD* result by measurements is a very challenging task. In order to validate the *CFD* model by results of flow measurements, the experimental procedure is represented by *CFD* simulation as follows:

• the calculation grid is cut off at matrix outlet so that a free jet appears

• a cold steady mass flow is impressed on only one exhaust runner, which effects the same Reynolds numbers as the hot peak mass flows according to Figure 5

Figure 6 shows the velocity distribution calculated for such a flow experiment with cold air flow.
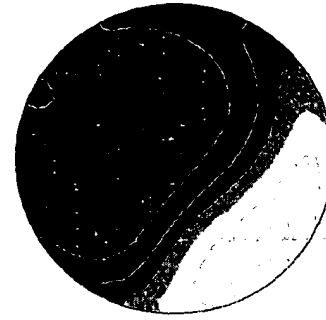

Figure 6. *CFD* Velocity Distribution at steady-state Cold Flow (Cylinder 3)

The comparison of the results presented in Figure 5 (cylinder 3) and Figure 6 shows that even with these significant simplifications the character of the velocity distribution on the catalyst front area remains nearly unchanged. Hence, the most important parameters for the catalyst flow distribution are the geometry of the ducts upstream and the flow resistance of the catalyst. This result not only permits the verification of the *CFD* calculation but also assures a high validity of the results determined at steady state conditions.

PIV MEASUREMENTS

As it proves all upstream effects in whole, the flow distribution measured at catalyst outlet is used to verify *CFD* results. *PIV* measurements are used to have a first insight into the flow field downstream of the brick.

The *PIV* measurement technique is a planar, non-intrusive, whole-field tracer method. The observation plane is defined by a thin laser light sheet. The air is seeded with small tracer particles, which follow the flow and scatter light passing the laser light sheet. By means of two successive laser pulses with short temporal delay particle displacements and thus local velocities are documented on a camera, positioned perpendicular to the light sheet, Figure 7.
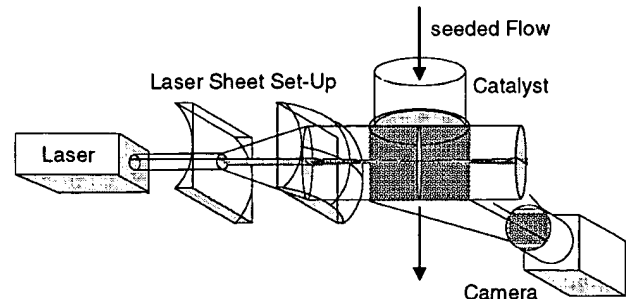

Figure 7. *PIV* Data Acquisition

Two separated frames, each single-exposed by one of the laser pulses, contain the local velocity information without directional ambiguity. In mathematical terms, the shift of the light intensity distribution between pairs of small "fields of view" - located at identical positions in both single exposed frames - is calculated by spatial

cross correlation. The resulting velocity data are validated by the correlation peak ratios. An average velocity field is calculated from 20 single recordings.

Figure 8 presents a typical result of the *PIV* investigations. The free jet downstream of the catalyst matrix at steady flow conditions is shown to be one-dimensional over a remarkable long distance.
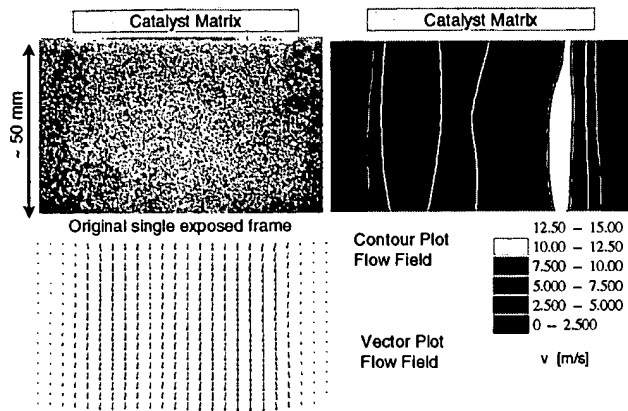

Figure 8.　Flow Field downstream Catalyst
(Steady Flow/ *PIV* Results)

In order to check the influence of the test conditions furthermore, Figure 9 varies the mass flow rate. The individual results are scaled to the corresponding flow rate.
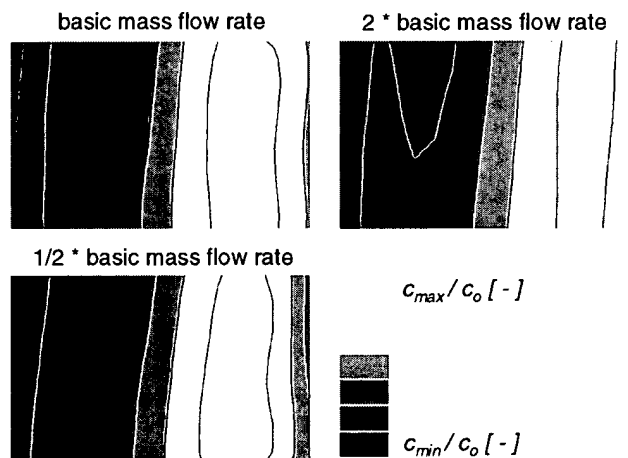

Figure 9.　Flow Field downstream Catalyst at different Mass Flow Rates (*PIV* Results)

Although the mass flow is halved and doubled respectively, the scaled results are extensively similar. This again ensures steady investigations a high validity.

HWA MEASUREMENTS

To record the complete mass flow distribution with *PIV* the catalyst outlet would have to be scanned by numerous shifted laser light sheets. Therefore *PIV* is not the first choice for this measurement task. As the *PIV* investigations demonstrate a dominant axial flow downstream catalyst it is possible to quantify the mass

flow distribution by means of a single hot wire probe, Figure 10. The flow field is scanned in successive steps.
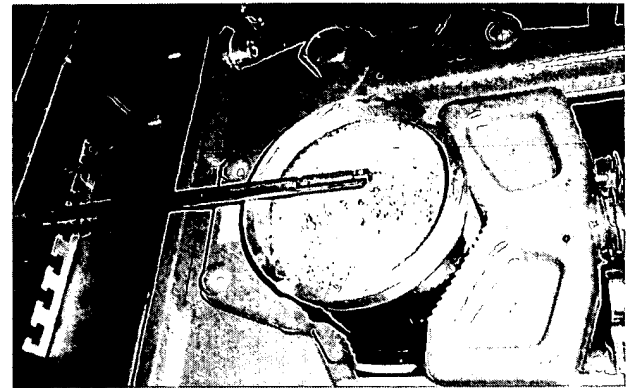

Figure 10.　Setup of *HWA* Testing

Figure 11 presents a comparison between *Hot Wire Anemometry* (*HWA*) and *PIV* at identical boundary conditions.
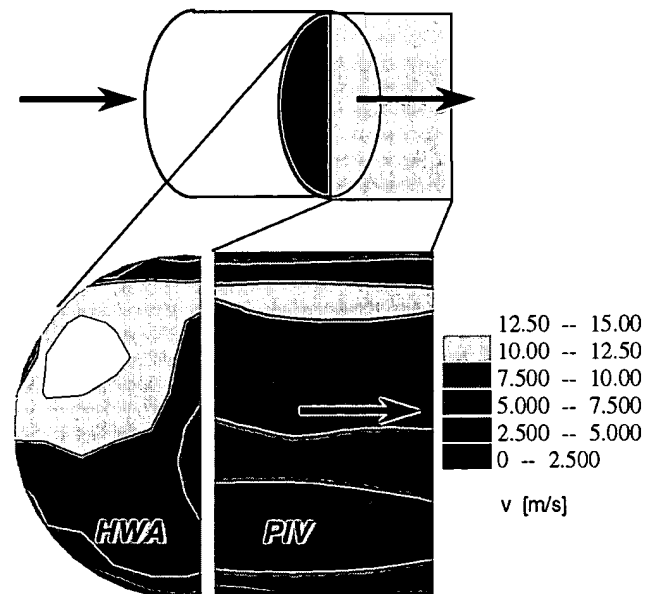
Figure 11.　Comparison *HWA/PIV* Results

The gap between catalyst outlet and probe is chosen in a manner, that avoids flow blocking by the sensor. Falsifying effects by the free jet expansion are minor critical.

The comparison demonstrates that *HWA* measurements are suitable to determine the flow distribution at the outlet of the catalyst matrix.

BOUNDARY CONDITIONS FOR *HWA* TESTING

Investigations so far showed that

- results determined at steady state, cold conditions in the free jet at catalyst outlet can be used well to characterize the real mass flow distribution inside the brick

- the steady results permit the verification of *CFD* calculations
- *HWA* is a suitable measurement technique for the determination of the mass flow distribution

In this chapter practical boundary conditions for *HWA* measurements are derived. The cold test mass flow (index *c*) should reproduce the *Re* numbers at hot operating conditions (index *h*):

$$Re_c = \frac{c_c D}{v_c} \overset{!}{=} Re_h = \frac{c_h D}{v_h}$$ {3}

Because of

$$\dot{m}_c = \rho_c A c_c; \quad \dot{m}_h = \rho_h A c_h$$ {4}

and equation {2} the cold mass flow has to be adjusted to

$$\dot{m}_c = \dot{m}_h \left(\frac{T_c}{T_h}\right)^{0,63}$$ {5}

The medium hot mass flow out of one cylinder is

$$\dot{m}_h = \lambda_a \rho_L V_h 2n$$ {6}

This formula is valid for non-overlapping exhaust strokes. In order to create a coherent reference basis for all engines the following full load values are defined:

$$\rho_L = 1.18 \frac{kg}{m^3}; \quad \lambda_a = 1$$

$$n = 6000 \frac{1}{min}; \quad \left(\frac{T_c}{T_h}\right) = 0,25$$ (7)

The cold mass flow according to {5}, {6} and {7} is fed through each individual exhaust runner. Figure 12 shows the measurement result corresponding to Figure 6. The correlation between calculation and experiment is clearly visible.

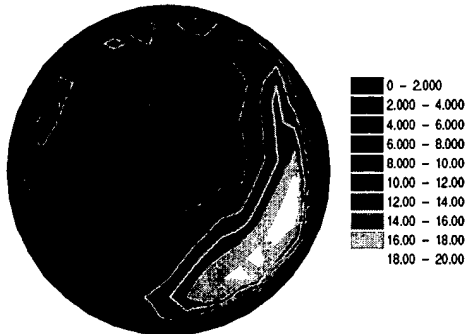|	
	0 - 2.000
	2.000 - 4.000
	4.000 - 6.000
	6.000 - 8.000
	8.000 - 10.00
	10.00 - 12.00
	12.00 - 14.00
	14.00 - 16.00
	16.00 - 18.00
	18.00 - 20.00

Figure 12. *HWA* Velocity Distribution (Cylinder 3)

ESTIMATION OF THE RESULTS

It is obvious that the results according to Figure 12 allow a deep insight into the flow distribution upstream of the catalyst matrix and are a start for geometric modifications. Nevertheless, based only upon the contour plots it is difficult to quantify the effects.

For quantification of the flow distribution two code numbers are well established. The standard deviation of the velocity distribution is given by

$$RMS = \sqrt{\frac{\sum_{i=1}^{N}\left\{\left[\left(\frac{c_i}{c_o}-1\right)^2\right]\right\}}{N}}$$ {8}

the uniformity index /4/ is defined as

$$\gamma = 1 - \frac{\sum_{i=1}^{N}\left|\frac{c_i}{c_o}-1\right|}{2N}$$ {9}

In both cases

$$c_o = \frac{\sum_{i=1}^{N} c_i}{N}$$ {10}

represents the average velocity. Figure 13 illustrates the actual meaning of these code numbers assuming three synthetic velocity distributions c/c_0 at a hypothetical 1D catalyst (length *L*).
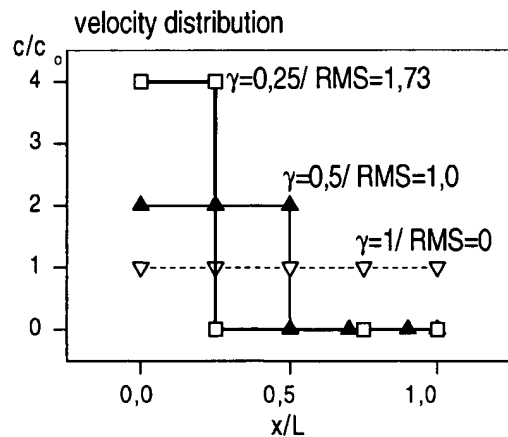

Figure 13. Meaning of Uniformity Numbers

Obviously the uniformity index describes the share of the catalyst area which is loaded effectively by the flow i.e. the area exploitation (looking to the x axis). The RMS value is a measure for the deviation from the average velocity (looking to the y axis).

Of course flow distributions which are entirely different can cause the same uniformity numbers. Thus, a characterization of the distribution only by scalar values is incomplete.

A compromise between flow assessment by 2D velocity distribution plots and by scalar code numbers is based upon the frequency distribution of the measured velocities c_i. The accumulated frequency fraction can be seen as a non-dimensional position and serves as normalized x-axis. The y-axis displays the corresponding flow velocity class, related to the mean value c_o.
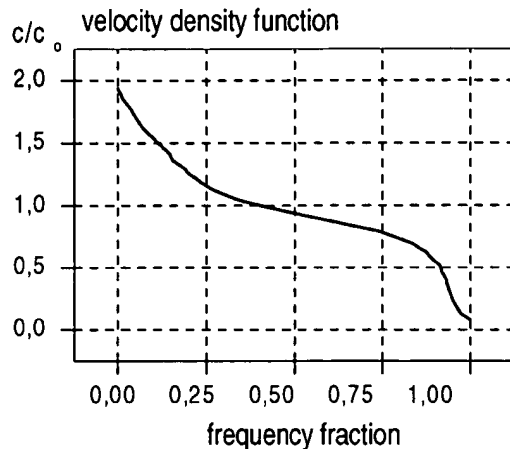

Figure 14. Velocity Density Function

Figure 14 shows a high similarity to Figure 13. The 2D result is reduced to a equivalent flow distribution of a hypothetical in-line converter, having the same uniformity and RMS index. The result reveals the range of velocity fluctuations, but does not show their actual locations any more.

In particular, this form of the velocity distribution allows the comparison of different concepts in a very effective way. The scalar code numbers are still contained implicitly in this plot.
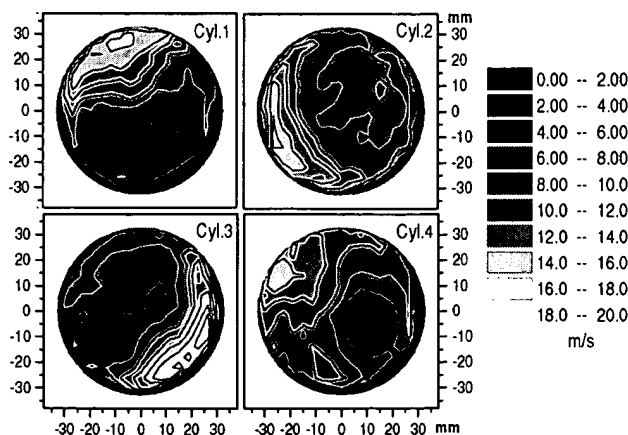

Figure 15. Cylinder-Individual HWA Results

EXAMPLE OF USE

In order to demonstrate the expressiveness of the velocity classification an analysis of a four-cylinder engine is shown. Figure 15 displays the primary, cylinder individual HWA results.

To get a first idea of the average flow situation, the individual results are superimposed, Figure 16. Additionally, the local minima and maxima as well as their differences are plotted. The latter one gives a first idea of the alternating stresses due to velocity spots.
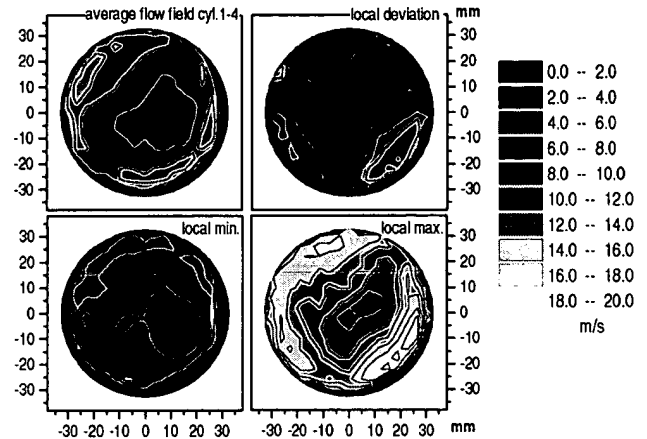

Figure 16. Composed HWA Results

Finally, the velocity density functions are calculated. This form allows a very instructive comparison of the individual flow fields. The difference between the average curve of the cylinder-individual results and the density function of the average flow field indicates, how the locations of velocity spots fluctuate with the cylinder load.
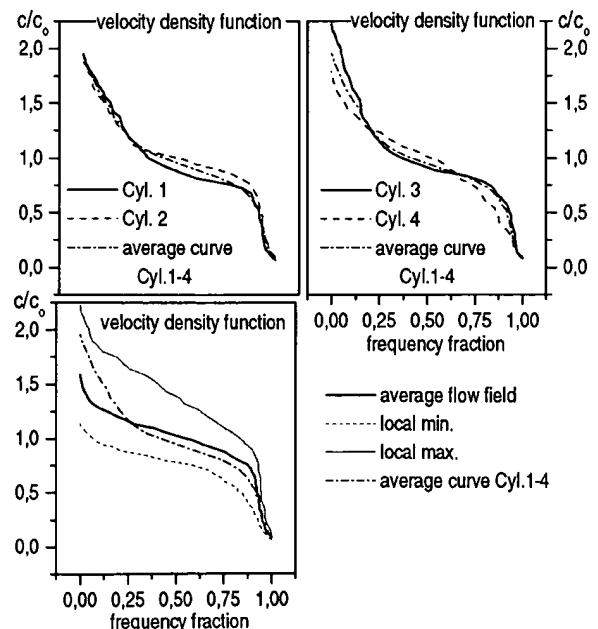

Figure 17. Velocity Density Functions

CONCLUSION

Measurements with *HWA* are suitable to determine uniform flow distribution at the outlet of a catalyst matrix in steady-state experiments. These investigations can not only be used to validate *CFD* results but are a start itself for system optimizations. The success of modifications can be shown very instructively by using the density function of the mass flow distribution.

ACKNOWLEDGMENTS

REFERENCES

1. S. Voeltz, A. Kuphal, S. Lieske, A. Fritz: "Der Abgaskrümmer-Vorkatalysator für die neuen 1,0l- und 1,4l-Motoren von Volkswagen", MTZ 60 (1999) 7/8

2. C. Schernus, S. Lieske, R. Krebs, A. Kuphal, S. Voeltz: "Flow Behaviour Development of Close Coupled Catalytic Converters", Aachen Colloquium Automobile and Engine Technology 1999

3. H. Bressler, D. Rammoser, H. Neumaier, F. Terres: "Experimental and Predictive Investigation of a Close Coupled Catalytic Converter with Pulsating Flow", SAE 960564, 1996

4. H. Weltens, H. Bressler, F.Terres, H. Neumaier, D. Rammoser: "Optimization of Catalytic Converter Gas Flow Distribution by CFD Prediction", SAE 930780, 1993

ACRONYMS, ABBREVIATIONS

CFD:	computational fluid dynamics
PIV:	particle image velocimetry
HWA:	hot wire anemometry
Ma:	Mach number
Re:	Reynolds number
Eu:	Euler number
xD:	x dimensional
Δp:	pressure drop
ρ:	density
c:	velocity
D:	(characteristic) diameter
v:	kinematic viscosity h/r
η:	dynamic viscosity
T:	temperature
$\dot{m}$:	mass flow rate
n:	engine speed
V_h:	cylinder displacement
λ_a:	volumetric efficiency
ρ_L:	density of air (intake conditions)
RMS:	root mean square value
γ:	uniformity index
c_i:	local velocity (*HWA* result)
c_o:	average velocity
N:	number of scanned points (*HWA*)
L:	length

7